HHS Public Access

Author manuscript

J Mater Chem B Mater Biol Med. Author manuscript; available in PMC 2017 October 28.

Published in final edited form as:

J Mater Chem B Mater Biol Med. 2016 October 28; 4(40): 6534–6540. doi:10.1039/C6TB01828A.

Recovery property of double-network hydrogel containing mussel-inspired adhesive moiety and nano-silicate†

Yuan Liu[a] and **Bruce P. Lee**[a]

[a]Department of Biomedical Engineering, Michigan Technological University, 1400 Townsend Dr, Houghton, MI, 49931, USA

Abstract

Altough double network (DN) hydrogels are extremly tough, they are irreversibly softened during large strain deformation. We incorporated mussel-inspired adhesive moiety, catechol, and a synthetic nano-silicate, Laponite, into DN to examine the effect of strong, reversible crosslinks on the DN's ability to recover its mechanical properties during successive loading cycles. The introduction of catechol and Laponite drastically increased the compressive strength and toughness of DN without compromising the compliance of the hydrogel. After 2 hours of recovery at room temperature, the nanocomposite DN hydrogel recovered over 95 and 82 % of its strain energy and hysteresis, respectively, during successive compressive loading to a strain of 0.5. Both equilibrium swelling and oscillatory rheometry data confirmed that there were minimal changes to the network crosslinking density and stiffness after large strain compressive deformation, indicating that mechanical loading did not result in irreversible structural damage. Strong catechol-Laponite interactions can be repeatedly broken and reform to dissipate fracture energy and enable the recovery of DN hydrogel.

Graphical Abstract

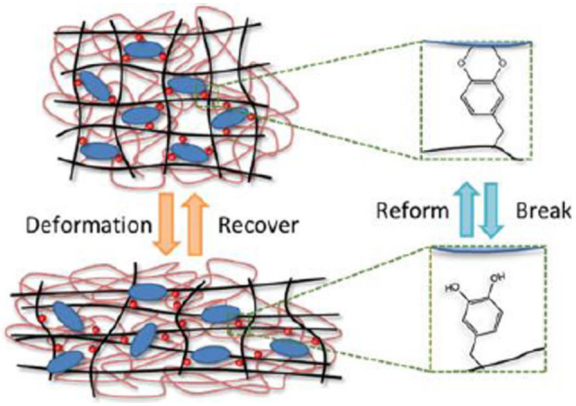

Adhesive catechol moiety and Laponite were incorporated into double network to form a mechanically tough and recoverable hydrogel. The ability for catechol-Laponite to repeatedly

†Electronic Supplementary Information (ESI) available: Additional mechanical testing results. See DOI: 10.1039/x0xx00000x

Correspondence to: Bruce P. Lee.

break and reform, dissipated fracture energy and minimized structural damage during large strain deformation.

Introduction

Hydrogel is a widely used biomaterial due to its excellent biocompatibility, diversity of functionality, and tunable material and physical properties. Hydrogels have been utilized as tissue engineering scaffolds,[1–4] tissue adhesives,[5, 6] biosensors,[7, 8] and soft actuators.[9–11] For many applications (e.g. repair of soft connective tissue), hydrogels are required to maintain their structural integrity while resisting large and repeated mechanical loading.[12, 13] Designing mechanically strong hydrogels with exceptional recovery properties remains a challenge.

Gong and co-workers[14, 15] developed a new type of interpenetrating network hydrogel, the so-called double network (DN) hydrogel, which exhibited remarkable high strength (10^6–10^7 Pa) and fracture toughness (10^2 to 10^3 J/m^2). Despite having high water contents (65–95 wt%), DN hydrogels exhibited fracture toughness similar to those of solvent free rubbers and connective tissues.[15, 16] DN is composed of a stiff, densely crosslinked first network, interpenetrated with a soft, loosely crosslinked second network. While these two networks are not suitable for mechanical loading in and of themselves, their unique combination yields a fracture resistant DN hydrogel that exhibits mechanical properties that are two to three orders of magnitude higher than those of the two individual networks comprising the DN.[14] However, this remarkable mechanical property is achieved at the expense of irreversible bond breakage within the hydrogel architecture, and a large deformation (> 0.2 strain) irreversibly softens DN hydrogels.[17, 18] The irreversible nature of DN may hinder its usage in applications where repeated, large strain load-bearing is required.

Recently, recoverable DN hydrogels composed of a physically crosslinked first network (i.e., alginate[19] and agarose[20]) have been reported. However, heating to elevated temperatures for extensive periods of time (i.e., 80°C for 1 day and 100°C for 30 min for alginate and agar, respectively) was needed for recovery, which is impractical for many applications. Additionally, only less than 70 % energy recovery was reported. Other recoverable DN hydrogels have not been able to replicate the elevated mechanical properties of DN.[21–23]

Marine mussels secrete adhesive proteins that enable these organisms to bind to different surfaces in a wet environment.[24, 25] These proteins contain a unique amino acid, 3,4-dihydroxyphenylalanine (DOPA), with a catechol side chain that is capable of binding to both organic and inorganic surfaces through either covalent crosslinking or strong reversible bonds.[26] Hydrogels constructed by catechol-metal ions complexation,[27, 28] catechol-boronate complexation,[29] and catechol-inorganic nanoparticles interfacial binding[30] have demonstrated self-healing property. Specifically, the reversible bond formed between a catechol and a metal surface averaged around 800 pN, reaching 40 % that of a covalent bond.[31] Our lab previously exploited this interaction to create nanocomposite hydrogels with improved strength and toughness by incorporating network-bound catechol and a nano-silicate, Laponite.[32–34] These nanocomposite hydrogels were capable of sustaining repeated large strain (0.8) deformation and recovery without fracturing.[32]

In this work, we tested the hypothesis that the incorporation of catechol and Laponite can be used to construct recoverable DN hydrogels. Both network-bound catechol and Laponite were introduced into the first network and the influence of catechol-Laponite interaction on the recovery property of the nanocomposite DN hydrogel was evaluated.

Experimental

Materials

Acrylamide (AAm) and 2-acrylamido-2-methyl-1-propanesulfonic acid (AMPS) were purchased from Sigma Aldrich (St. Louis, MO). *N,N'*-Methylene-bisacrylamide (MBAA) and 2,2-dimethoxy-2-phenylacetophenone (DMPA) were obtained from Acros Organics (Geel, Belgium). Dimethyl sulfoxide (DMSO) was purchased from Fisher Scientific Co. (Pittsburgh, PA). Dopamine methacrylamide (DMA), which contained the adhesive catechol and polymerizable methacrylate group, was synthesized as previously described.[35] Laponite XLG was a gift from Southern Clay Products, Inc. (Austin, TX).

Synthesis of hydrogel

The double network hydrogels were prepared in two steps. To prepare the first network, Laponite, AAm, and AMPS were dissolved in deionized water. DMA and MBAA were dissolved in an aqueous solution containing 50 % DMSO. DMPA was dissolved in anhydrous ethanol at 10 mg/ml. These three solutions were mixed together to give the precursor solution for the first network, and the combined monomer (AAm/AMPS/DMA) concentration was kept at 1 M in the precursor solution. The concentration of AAm and AMPS were kept at equimolar while the concentration of DMA was kept at either 0–10 mol % relative to the total concentration of the monomers. The crosslinker (MBAA) and the photoinitiator (DMPA) were kept at 4 and 0.1 mol%, respectively, relative to the monomers. Laponite was kept at 0–4 wt% in the precursor solution. The precursor solution was deoxygenated with three vacuum-nitrogen purge cycles[32] and photo-irradiated for 2.5 h in a mould consisting of two glass plates separated by 1.5 mm thick rubber spacer using a UV crosslinker (XL-1000, Spectronics Corporation, Westbury, NY) located in a nitrogen-filled glove box (830-ABB Plas-Labs, Lansing, MI). The first network hydrogels were denoted using the notation DxLy, where x is the mol % of the DMA relative to monomer and y is the wt% of Laponite.

The first network hydrogel was submerged in the degassed second network precursor solution, composed of 2 M AAm, 0.1 mol % MBAA and DMPA for 24 h. The swollen hydrogel that was infused with the second network precursor solution was photo-irradiated for 2.5 h in a nitrogen-filled glove box. DN hydrogels were denoted using the notation DxLy/DN. A second network composed of PAAm was also synthesized by photo-irradiating the precursor solution.

Hydrogel characterization

Fourier transform infrared (FTIR) spectra of the dried samples were obtained using a Perkin Elmer Spectrum One spectrometer. Equilibrium water content (EWC) was determined by

incubating the hydrogels in mildly acidic water (pH = 3.5) and vacuum-dried for 2 days. EWC was defined as:

$$EWC = \frac{M_s - M_d}{M_s} \times 100\% \quad (1)$$

where M_s and M_d are the mass of swollen and dried hydrogels, respectively. The mass ratio between the second network and the first network within a DN (R_{mass}) was defined as:

$$R_{mass} = \frac{M_{DN} - M_{FN}}{M_{FN}} \quad (2)$$

where M_{FN} and M_{DN} denote the average dry mass of the first network and its corresponding DN hydrogel, respectively.

Compression testing

Unconfined, uniaxial compression testing was performed using an ElectroForce 3200 Series III Test Instrument (Bose Corporation, Eden Prairie, MN, USA). Hydrogels (n = 3) were compressed at a rate of 1.8 mm/min until the sample fractured. The dimensions of each hydrogel (diameter ~ 7 mm; thickness ~ 3 mm) were measured using a digital caliper immediately before testing. Stress was determined based on the measured load divided by the initial surface area of the sample. Strain was determined by dividing the change in the position of the compressing plate by the initial thickness of the hydrogel. Toughness was determined by the integral of the stress-strain curve. The elastic modulus was taken from the slope of the stress-strain curve between a strain of 0.05 and 0.15.

The maximum stress normalized by the mass of second network in DN (σ_{normal}) was determined by:[18]

$$\sigma_{normal} = \frac{\sigma_{original}}{r^{2/3}} \quad (3)$$

where $\sigma_{original}$ is the experimentally determined maximum stress of DN and r is the mass fraction of second network in DN, which is determined by:

$$r = \frac{M_{DN}}{M_s} \times \frac{R_{mass}}{R_{mass}+1} \quad (4)$$

For repeated cyclic loading, hydrogels were compressed to a strain of 0.5 and unloaded to 0 strain at a fixed rate of 0.85 mm/min with a wait time of 0 or 2 h between cycles. Strain energy was determined by the area under the loading portion of the stress-strain curve. The energy dissipated during each cycle was determined by finding the area of hysteresis within

a cycle of the stress-strain curve. The % recovery was calculated as defined by the ratio of the values found in the 2nd loading cycle divided by those found in the 1st cycle.

Effect of compressive loading on hydrogel equilibrium volume

Hydrogels were subjected to compressive cyclic loading to a strain of 0.5 at a rate of 0.85 mm/min and allowed to re-equilibrate in mildly acidic water (pH = 3.5) for 24 h. The hydrogel volumetric ratio $\boldsymbol{R_{volume}}$ was determined by:

$$R_{\text{volume}} = \frac{V_{\text{after compression}}}{V_{\text{virgin}}} \quad (5)$$

where $\boldsymbol{V_{virgin}}$ and $\boldsymbol{V_{after\ compression}}$ denote the hydrogel equilibrium volume for the virgin hydrogel and a hydrogel subjected to compressive loading cycle, respectively. The equilibrium volume of hydrogel in each state was determined by:

$$V = \frac{M_{\text{p}}}{\rho_{\text{p}}} + \frac{M_{\text{lap}}}{\rho_{\text{lap}}} + \frac{M_{\text{H}_2\text{O}}}{\rho_{\text{H}_2\text{O}}} \quad (6)$$

where $\boldsymbol{M_p}$, $\boldsymbol{M_{lap}}$, $\boldsymbol{M_{H_2O}}$ are the mass of the polymer matrix, Laponite, and water, respectively. $\boldsymbol{\rho_p}$ is the density of polymer (1.3 g/cm^3),[36] $\boldsymbol{\rho_{lap}}$ is the density of Laponite (2.53 g m/cm^3),[37] and $\boldsymbol{\rho_{H_2O}}$ is the density of water (1 g/cm^3). $\boldsymbol{M_{H_2O}}$ was determined from subtracting the dried mass of hydrogel ($\boldsymbol{M_d}$) from its swollen mass ($\boldsymbol{M_s}$). Both $\boldsymbol{M_d}$ and $\boldsymbol{R_{mass}}$ were used to calculate $\boldsymbol{M_p}$ and $\boldsymbol{M_{lap}}$ based on the theoretical wt% of Laponite used in the precursor solution in the first network.

Effect of compressive loading on rheological properties

Rheological properties of virgin hydrogels and those that were previously subjected to a compressive loading cycle (strain = 0.5, rate = 0.85 mm/min) were characterized using a HR-2 rheometer (TA Instruments, New Castile, DE, USA). A frequency sweep (0.1 – 20 Hz at 0.1 strain) experiment was performed to determine the storage (G') and loss (G") moduli. Hydrogel discs (diameter ~ 8 mm, n = 3) were tested using parallel plates at a gap distance that is set at 90 % that of the individual hydrogel thickness, as measured by a digital caliper.

Statistical analysis

Statistical analysis was performed using Origin Pro software. Student t-test and One-way analysis of variance (ANOVA) with Tukey HSD analysis were performed for comparing means of two and multiple groups, respectively, using a p-value of 0.05.

Results and Discussion

Nanocomposite DN hydrogels containing Laponite and network-bound catechol groups were prepared. Catechol and Laponite were incorporated into the first network (FN) to introduce reversible crosslinking into the DN. Given that catechol readily undergoes auto-

oxidation in a basic condition, hydrogels were equilibrated in a mildly acidic aqueous solution (pH = 3.5) to preserve the reduced and adhesive form of the catechol side chain for our experiments.[34, 38]

Hydrogel characterization

FTIR spectra (Fig. 1) confirmed the presence of catechol and Laponite in the nanocomposite DN hydrogels. The spectrum of PAAm exhibited feature bands at 1645 cm^{-1} for C=O, 3326 cm^{-1} and 3188 cm^{-1} for primary $–NH_2$, 2929 cm^{-1} and 1447 cm^{-1} for $–CH_2–$, confirming the presence of acrylamide. The band at 1037 cm^{-1} of D0L0 was assigned to the S=O stretching of SO_3H in AMPS. In addition to PAAm and AMPS features, D10L2/DN also exhibited characteristic peaks at 988 and 1529 cm^{-1} for the Si-O-Si stretching of Laponite and the benzene ring of catechol, respectively.

The FN hydrogel, D0L0, was highly swollen with a EWC of over 99 wt% due to the highly charged AMPS side chain (Table 1). The addition of only Laponite (D0L2) and DMA (D10L0) marginally decreased the hydrogel water content when compared to D0L0, which is attributed to the interfacial interaction between Laponite and polymer matrix[39, 40] and intermolecular interactions (i.e., **π-π** interaction, hydrogen bonding)[25, 41] between network-bound catechol groups, respectively. When the DMA concentration was fixed at 10 mol%, increasing the Laponite concentration from 0 to 4 wt% significantly decreased the EWC of hydrogels. A similar trend was observed when the DMA concentration was increased from 0 to 10 mol% while keeping the Laponite concentration fixed at 2 wt%. Strong catechol-Laponite interactions resulted in the formation of new crosslinking points within the network, causing these hydrogels to deswell.

The EWC for DN was significantly lower when compared to values for the corresponding FN due to the infiltration of a second network. Additionally, the mass ratio between the second and first networks of DN ($\boldsymbol{R}_{\mathbf{mass}}$) varied proportionally with the EWC of the first network. The ability for the first network to swell allowed more of the second network monomer to infiltrate into the first network, resulting in a higher $\boldsymbol{R}_{\mathbf{mass}}$ value. As such, incorporating both DMA and Laponite drastically reduced $\boldsymbol{R}_{\mathbf{mass}}$ value.

Unconfined compression testing

The representative compressive stress-strain curves for the first network hydrogel containing 10 mol % DMA and 2 wt% Laponite (D10L2), the polyacrylamide second network (PAAm), and the corresponding DN hydrogel (D10L2/DN) are shown in Fig. 2. The densely crosslinked D10L2 behaved as a brittle polymer network, while PAAm was loosely crosslinked and significantly more compliant. The combination of these two polymer networks resulted in a tough DN, which exhibited mechanical properties that were more than an order of magnitude higher when compared to the individual networks used to form the DN (Table S1, Fig. 3). For example, the toughness of D10L2/DN was measured to be 67 and 24 times higher when compared to those measured for D10L2 and PAAm, respectively. This indicated that we have successfully prepared DN containing catechol and Laponite.

Laponite interacted weakly to the hydrogel matrix.[39, 40] At the concentrations tested, incorporation of Laponite alone (D0L2/DN) did not significantly increase its mechanical properties when compared to D0L0/DN (Fig. 3). On the other hand, when 10 mol% of DMA alone was introduced (D10L0/DN), max stress, elastic modulus, and toughness were moderately enhanced. This observation demonstrated that intermolecular interactions between network-bound catechol groups contributed to enhanced the mechanical properties of DN.

When the Laponite content in first network was fixed at 2 wt%, the mechanical properties of DN were significantly enhanced when DMA concentration was increased from 0 to 10 mol % (Fig. S1). Among the formulations tested, D10L2/DN exhibited the highest max stress (6.1 ± 0.11 MPa) and toughness (1200 ± 26 kJ/m^3). This increase in the mechanical properties coincided with an increase in its first network hydrogel (D10L2) when compared to those without both DMA and Laponite (i.e., D0L0, D0L2, and D10L2; Table S1). Our data confirmed previously published results, where the elastic modulus of the first network greatly influences the mechanical properties of the corresponding DN hydrogels.[42, 43] This increase in mechanical properties did not compromise the compliance of D10L2/DN.

Further increase in Laponite content resulted in a stiff but brittle DN (i.e., D10L4/DN). D10L4 had the lowest EWC among all the first network formulation tested due to extensive physical crosslinking between catechol and Laponite (Table 1). This prevented swelling and diffusion of monomers into D10L4, resulting in the lowest second network mass ratio ($\boldsymbol{R}_{\mathbf{mass}}$ = 2.4). The ductile second network prevents macroscopic crack propagation through viscous dissipation.[14] To obtain DN with elevated toughness, the molar concentration of the second network is required to be 20–30 times that of the first network ($\boldsymbol{R}_{\mathbf{mass}}$ ~ 7–10).[14, 15] The presence of the negatively charged AMPS in the first network promoted its swelling and diffusion of second network monomers into the first network to ensure a large $\boldsymbol{R}_{\mathbf{mass}}$ value. However, strong interaction between catechol and Laponite in D10L4 counteracted the swelling promotion effect of AMPS, and resulted in low second network content in D10L4/DN with significantly reduced toughness.

Given that the amount of second network varied in different DN formulations, the maximum stress of DN was normalized by the mass fraction of the second network ($\boldsymbol{\sigma}_{\mathbf{normal}}$, Table S2). $\boldsymbol{\sigma}_{\mathbf{normal}}$ values for D5L2/DN and D10L2/DN were 1.26 and 1.35 fold higher when compared to that of D0L0/DN, indicating that strong DMA-Laponite interactions contributed to the enhanced mechanical properties. On the other hand, adding Laponite alone (e.g., D0L2/DN) exhibited no enhancement in the maximum stress. Interestingly, adding DMA alone (e.g., D10L0/DN) also demonstrated an increase in the calculated $\boldsymbol{\sigma}_{\mathbf{normal}}$ value, indicating that intermolecular interaction between network bout catechol also contributed to the enhanced mechanical properties of DN.

Recovery property of DN during successive compressive loading

D0L0/DN and D10L2/DN were chosen to conduct cyclic compression testing with or without wait time between loading cycles (Table 2). Fig. 4 shows the representative stress-strain curves of D10L2/DN and D0L0/DN during two successive testing cycles with 2 h wait time. D0L0/DN exhibited a significant decrease in the measured strain energy and hysteresis

in the 2nd testing cycle and the % recovery of these values did not change with increasing wait time. This indicated that compressive loading irreversibly damaged D0L0/DN. On the other hand, when D10L2/DN was allowed to recover after the 1st loading cycle, there was a dramatic increase in the recovered strain energy and hysteresis (82 and 95 %, respectively) when compared to those measured without wait time (73 and 49 %, respectively).

The equilibrium volumes of hydrogel before (virgin) and after compression were measured to determine the effect of deformation on the network architecture (Fig. 5). For samples that do not contain both DMA and Laponite (i.e., D0L0/DN, D0L2/DN, and D10L0/DN), compressive loading resulted in structural damage and an increase in the equilibrium volume of these networks by more than 30 % ($\boldsymbol{R}_{\mathbf{volume}}$ ~ 1.3). Although these networks did not fracture macroscopically, deformation led to irreversible covalent bond breakage in the first network, and these fractured first network pieces were held together by the loosely crosslinked PAAm network.[43, 44] When these gels were allowed to re-equilibrate in a water bath, water diffused into the hydrogel network to cause an increase in its volume (Fig. 6). Conversely, the change in the equilibrium volume of D10L2/DN was significantly lower ($\boldsymbol{R}_{\mathbf{volume}}$ = 1.1±0.050, Fig. 5), indicating that there was minimal structural damage to D10L2/DN as a result of compressive loading.

Similarly, oscillatory rheometry was performed to determine the changes in the viscoelastic properties of DN before and after compression (Fig. 7). D0L0/DN exhibited a nearly 3 fold reduction in the measure G' values, indicating a reduction in crosslinking density after compression. Similarly, G" values of D0L0/DN was also reduced after compression (Fig. S2), which further indicated irreversible breakage of covalent bonds within the polymer network.[45, 46] On the other hand, there was no significant difference between the measured G' and G" values between the virgin D10L2/DN and those that were compressed to a strain of 0.5. This result further confirmed that the presence of DMA and Laponite minimized changes to the mechanical properties and the architecture of the DN hydrogel.

Collectively, our results confirmed that large strain deformation led to irreversible damage of conventional DN hydrogels.[47] The presence of the negatively charged AMPS in the first network stiffens its polymer chains for mechanical loading and the covalent bond breakage within its backbone dissipates energy and contributes to the toughening of DN.[43, 44] However, these damages were not recoverable and resulted in the irreversibly softening of the DN. As such, these conventional DN are not suitable for repeated, large strain deformation. Conversely, incorporating DMA and Laponite into the first network, introduced strong reversible crosslinks within DN. The binding energy between catechol and silica oxide is estimated to be 33 kCal/mol.[48] Although this is significantly lower when compared to that of a carbon-carbon (C-C) covalent bond (85 kcal/mol),[49] the interaction between catechol and Laponite is reversible. DMA-Laponite bonds were broken during the initial loading cycle, which dissipated fracture energy. These interfacial bonds reformed over time, which contributed to the recovery of the measured mechanical properties. This recovery is much faster when compared to previously reported recoverable DN and can be acheived without the need for heating.[19, 20]

Conclusion

In this work, we prepared DN hydrogel composed of DMA and Laponite within its first network. This nanocomposite DN hydrogel exhibited enhanced mechanical properties when compared to DN that do not contain both DMA and Laponite. The reversible DMA-Laponite bonds were broken under compressive loading, which dissipated fracture energy. When the nanocomposite DN were allowed to recover, DMA-Laponite bonds reformed and the hydrogel recovered over 82% of energy dissipated during successive loading cycles. In addition, both the equilibrium volume and oscillatory rheological data demonstrated that these gels exhibited minimal changes to the architecture and stiffness of the network after compression.

Supplementary Material

Refer to Web version on PubMed Central for supplementary material.

Acknowledgments

This project was supported by National Institutes of Health under the award number R15GM104846. YL was supported in part by the Doctoral Finishing Fellowship provided by the Graduate School at Michigan Technological University. The authors thank Shari Konst for her assistance with DMA synthesis.

References

1. Drury JL, Mooney DJ. Biomaterials. 2003; 24:4337–4351. [PubMed: 12922147]
2. Lee KY, Mooney DJ. Chemical Reviews. 2001; 101:1869–1879. [PubMed: 11710233]
3. Liu WG, Deng C, McLaughlin CR, Fagerholm P, Lagali NS, Heyne B, Scaiano JC, Watsky MA, Kato Y, Munger R, Shinozaki N, Li FF, Griffith M. Biomaterials. 2009; 30:1551–1559. [PubMed: 19097643]
4. Torres-Rendon JG, Femmer T, De Laporte L, Tigges T, Rahimi K, Gremse F, Zafarnia S, Lederle W, Ifuku S, Wessling M, Hardy JG, Walther A. Advanced Materials. 2015; 27:2989–2995. [PubMed: 25833165]
5. Liu XJ, Li HQ, Zhang BY, Wang YJ, Ren XY, Guan S, Gao GH. Rsc Advances. 2016; 6:4850–4857.
6. Murphy JL, Vollenweider L, Xu FM, Lee BP. Biomacromolecules. 2010; 11:2976–2984. [PubMed: 20919699]
7. Hong SM, Sycks D, Chan HF, Lin ST, Lopez GP, Guilak F, Leong KW, Zhao XH. Advanced Materials. 2015; 27:4035–4040. [PubMed: 26033288]
8. Zhai DY, Liu BR, Shi Y, Pan LJ, Wang YQ, Li WB, Zhang R, Yu GH. Acs Nano. 2013; 7:3540–3546. [PubMed: 23472636]
9. Lee BP, Konst S. Advanced Materials. 2014; 26:3415–3419. [PubMed: 24596273]
10. Zheng WJ, An N, Yang JH, Zhou JX, Chen YM. Acs Applied Materials & Interfaces. 2015; 7:1758–1764. [PubMed: 25561431]
11. Lee BP, Narkar A, Wilharm R. Sensors and Actuators B-Chemical. 2016; 227:248–254.
12. Bodugoz-Senturk H, Macias CE, Kung JH, Muratoglu OK. Biomaterials. 2009; 30:589–596. [PubMed: 18996584]
13. Stella JA, D'Amore A, Wagner WR, Sacks MS. Acta Biomaterialia. 2010; 6:2365–2381. [PubMed: 20060509]
14. Gong JP, Katsuyama Y, Kurokawa T, Osada Y. Advanced Materials. 2003; 15:1155–1158.
15. Tanaka Y, Kuwabara R, Na Y-H, Kurokawa T, Gong JP, Osada Y. The Journal of Physical Chemistry B. 2005; 109:11559–11562. [PubMed: 16852418]
16. Hagiwara Y, Putra A, Kakugo A, Furukawa H, Gong JP. Cellulose. 2010; 17:93–101.

17. Na YH, Tanaka Y, Kawauchi Y, Furukawa H, Sumiyoshi T, Gong JP, Osada Y. Macromolecules. 2006; 39:4641–4645.
18. Myung D, Koh WU, Ko JM, Hu Y, Carrasco M, Noolandi J, Ta CN, Frank CW. Polymer. 2007; 48:5376–5387.
19. Sun J-Y, Zhao X, Illeperuma WRK, Chaudhuri O, Oh KH, Mooney DJ, Vlassak JJ, Suo Z. Nature. 2012; 489:133–136. [PubMed: 22955625]
20. Chen Q, Zhu L, Zhao C, Wang Q, Zheng J. Advanced Materials. 2013; 25:4171–4176. [PubMed: 23765594]
21. Bakarich SE, Pidcock GC, Balding P, Stevens L, Calvert P, Panhuis MIH. Soft Matter. 2012; 8:9985–9988.
22. Stevens L, Calvert P, Wallace GG, Panhuis MIH. Soft Matter. 2013; 9:3009–3012.
23. Harrass K, Kruger R, Moller M, Albrecht K, Groll J. Soft Matter. 2013; 9:2869–2877.
24. Yamamoto H. Biotechnology and Genetic Engineering Reviews, Vol 13. 1996; 13:133–165.
25. Waite JH. International Journal of Adhesion and Adhesives. 1987; 7:9–14.
26. Lee BP, Messersmith PB, Israelachvili JN, Waite JH. Annual Review of Materials Research, Vol 41. 2011; 41:99–132.
27. Holten-Andersen N, Harrington MJ, Birkedal H, Lee BP, Messersmith PB, Lee KYC, Waite JH. P Natl Acad Sci USA. 2011; 108:2651–2655.
28. Hou S, Ma PX. Chem Mater. 2015; 27:7627–7635. [PubMed: 26834315]
29. He LH, Fullenkamp DE, Rivera JG, Messersmith PB. Chem Commun. 2011; 47:7497–7499.
30. Li QC, Barret DG, Messersmith PB, Holten-Andersen N. Acs Nano. 2016; 10:1317–1324. [PubMed: 26645284]
31. Lee H, Scherer NF, Messersmith PB. Proceedings of the National Academy of Sciences of the United States of America. 2006; 103:12999–13003. [PubMed: 16920796]
32. Skelton S, Bostwick M, O'Connor K, Konst S, Casey S, Lee BP. Soft Matter. 2013; 9:3825–3833.
33. Liu Y, Meng H, Konst S, Sarmiento R, Rajachar R, Lee BP. Acs Applied Materials & Interfaces. 2014; 6:16982–16992. [PubMed: 25222290]
34. Ding X, Vegesna GK, Meng H, Winter A, Lee BP. Macromolecular chemistry and physics. 2015; 216:1109–1119. [PubMed: 26929588]
35. Lee H, Lee BP, Messersmith PB. Nature. 2007; 448:338–341. [PubMed: 17637666]
36. Bicerano, J. Prediction of polymer properties. CRC Press; 2002.
37. Cummins HZ. Journal of Non-Crystalline Solids. 2007; 353:3891–3905.
38. Yu J, Wei W, Menyo MS, Masic A, Waite JH, Israelachvili JN. Biomacromol. 2013; 14:1072–1077.
39. Li P, Kim NH, Siddaramaiah, Lee JH. Compos Part B-Eng. 2009; 40:275–283.
40. Li P, Siddaramaiah, Kim NH, Heo SB, Lee JH. Composites Part B-Engineering. 2008; 39:756–763.
41. Waiter JH. Annals of the New York Academy of Sciences. 1999; 875:301–309. [PubMed: 10415577]
42. Gong JP. Soft Matter. 2010; 6:2583–2590.
43. Xin H, Saricilar SZ, Brown HR, Whitten PG, Spinks GM. Macromolecules. 2013; 46:6613–6620.
44. Brown HR. Macromolecules. 2007; 40:3815–3818.
45. Pettignano A, Häring M, Bernardi L, Tanchoux N, Quignard F, Díaz DD. Materials Chemistry Frontiers. 2017
46. Mukherjee S, Hill MR, Sumerlin BS. Soft matter. 2015; 11:6152–6161. [PubMed: 26143752]
47. Webber RE, Creton C, Brown HR, Gong JP. Macromolecules. 2007; 40:2919–2927.
48. Mian SA, Saha LC, Jang J, Wang L, Gao XF, Nagase S. Journal of Physical Chemistry C. 2010; 114:20793–20800.
49. Berg, JM., Tymoczko, JL., Stryer, L. Biochemistry, Fifth Edition. W. H. Freeman; 2002.

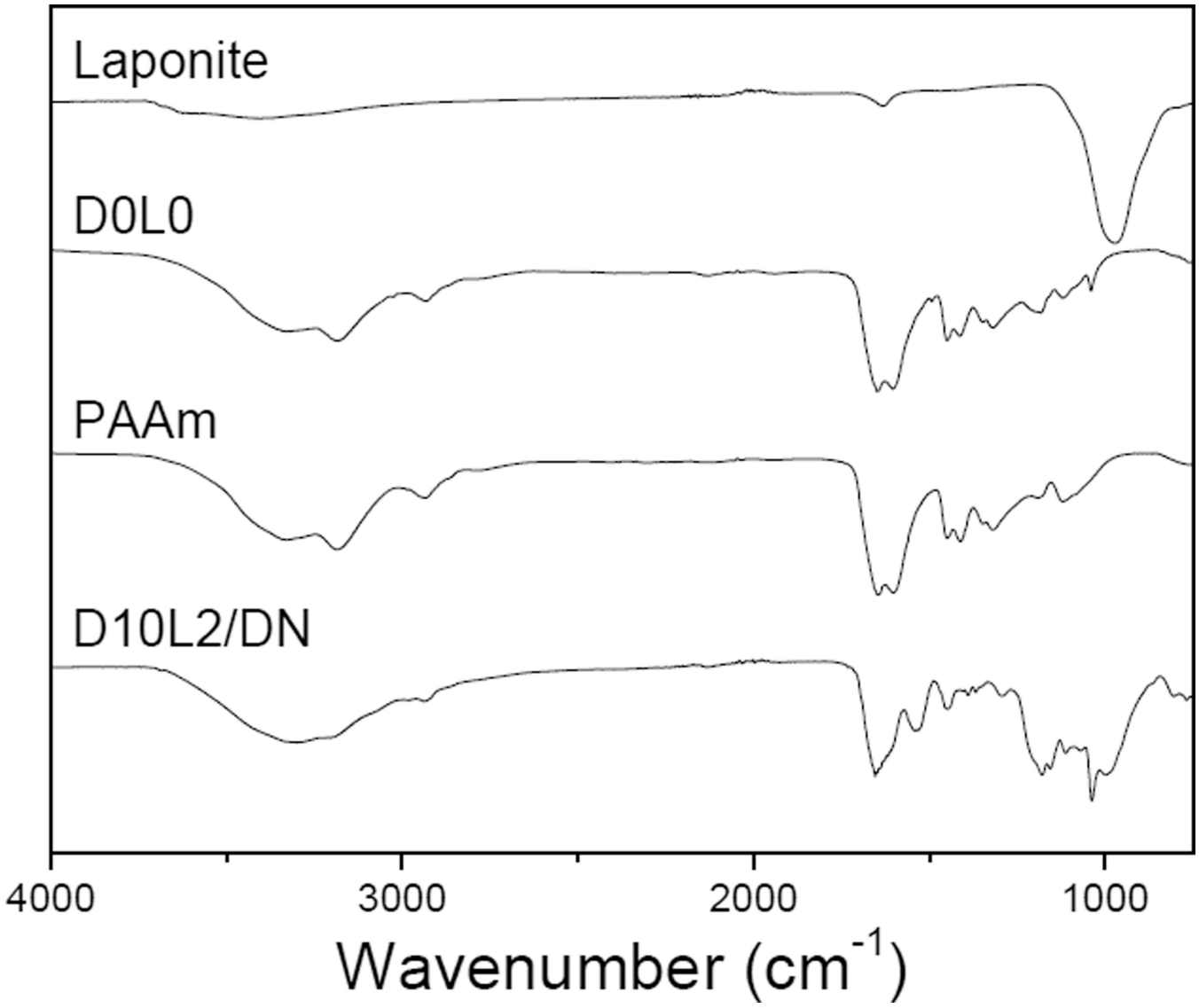

Fig. 1.
FTIR spectra of Laponite, D0L0, PAAm, and D10L2/DN.

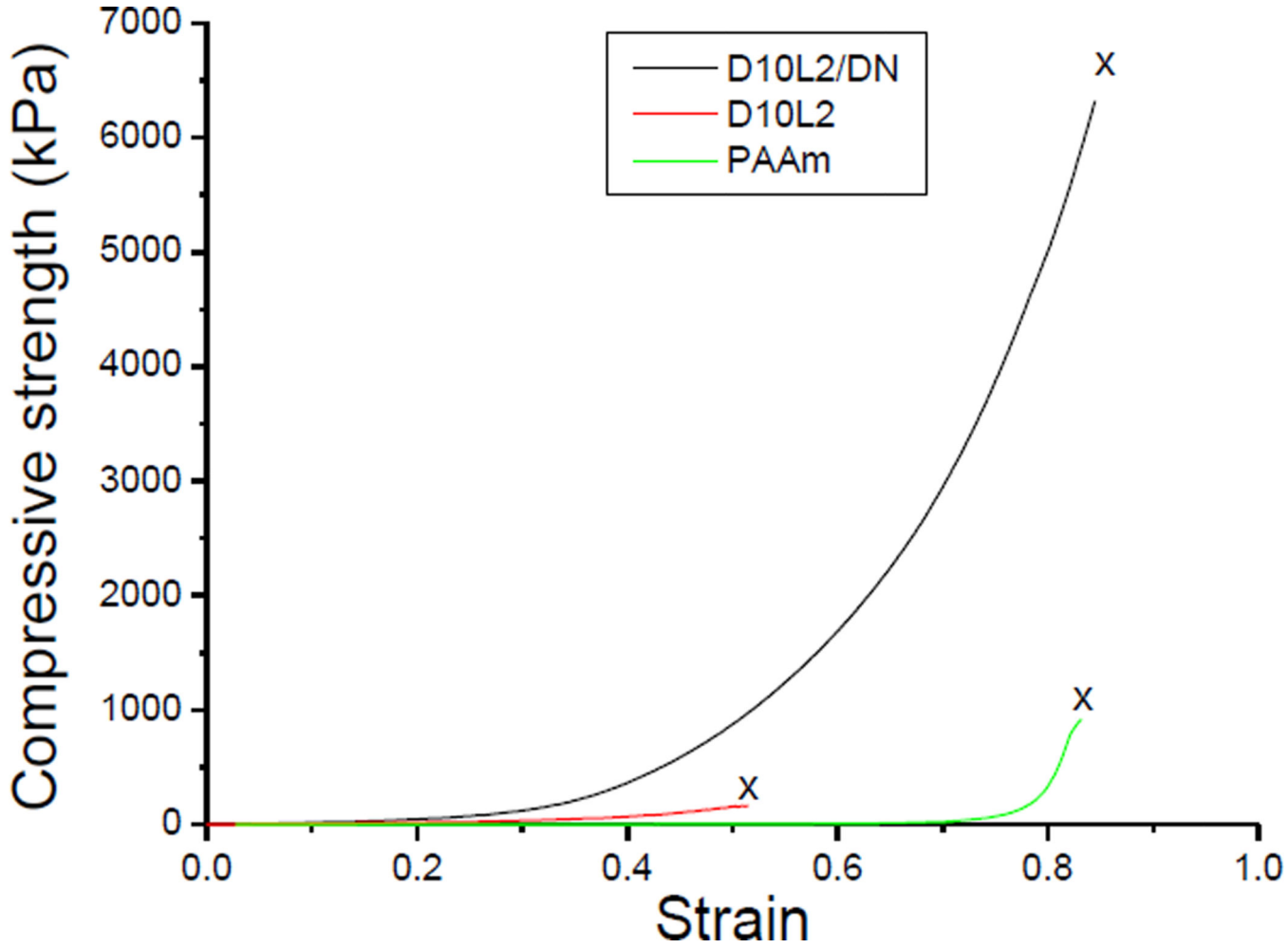

Fig. 2.

Representative stress-strain curves for the first network (D10L2), the second network (PAAm), and corresponding double network (D10L2/DN) hydrogels under unconfined uniaxial compression testing. “x” marks the indicate fracture point.

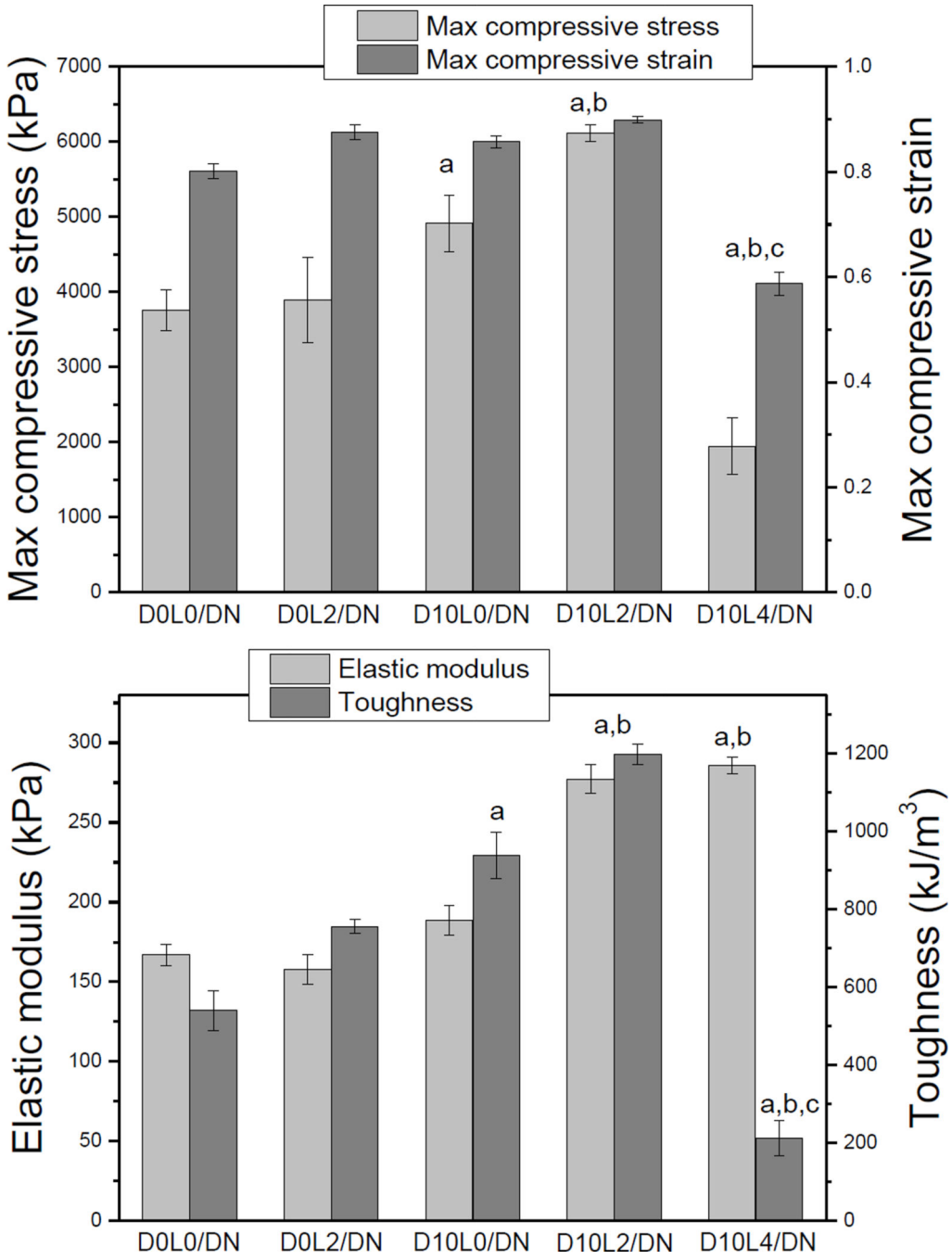

Fig. 3.

Measured compressive strength, strain, elastic modulus, and toughness of DN hydrogels. Data is presented as mean ± SD (n = 3). [a]$p < 0.05$ when compared to D0L0/DN and D0L2/DN, [b]$p < 0.05$ when compared to D10L0/DN, [C]$p < 0.05$ when compared to D10L2/DN.

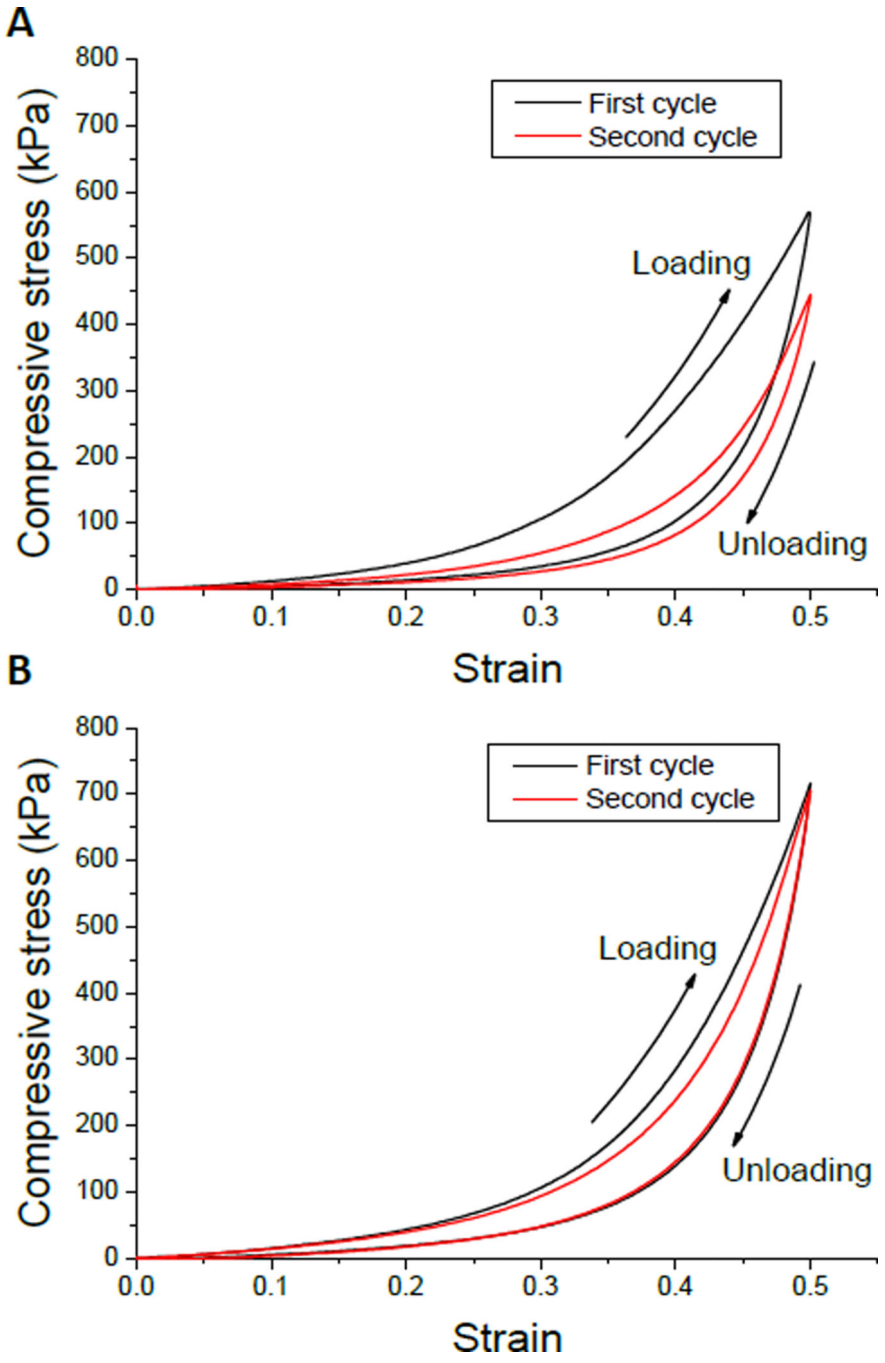

Fig. 4.

Representative stress-strain curves of the 1st (black) and 2nd (red) loading cycles in unconfined uniaxial compression for D0L0/DN (**A**) and D10L2/DN (**B**) hydrogels. The hydrogels were compressed to a strain of 0.5 and unloaded back to 0 strain. The gel samples were allowed to recover in mildly acidic water bath (pH = 3.5) for 2 hours at room temperature between cycles.

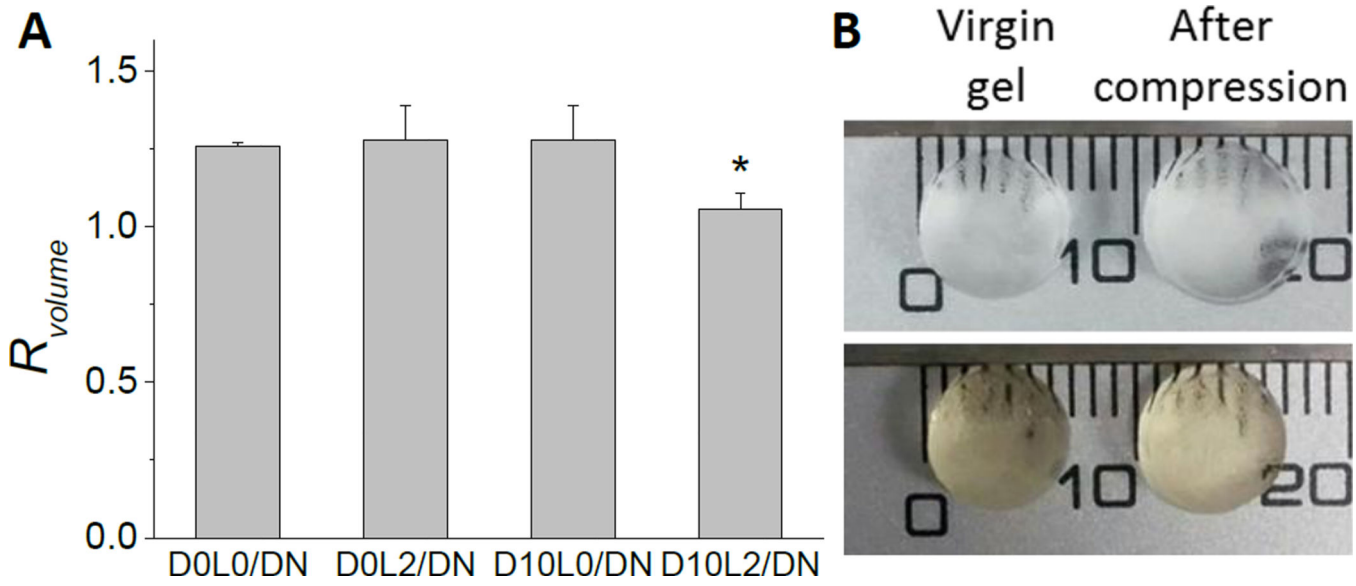

Fig. 5.

The ratio of the volume ($\boldsymbol{R_{volume}}$) of DN after compression to a strain of 0.5 when compared to virgin DN (**A**). Data is presented as mean ± SD (n=3). *p<0.05 when compared to D0L0/DN, D0L2/DN, and D10L0/DN. Photographs of D0L0/DN (top) and D10L2/DN (bottom) in the virgin state and after compression (B).

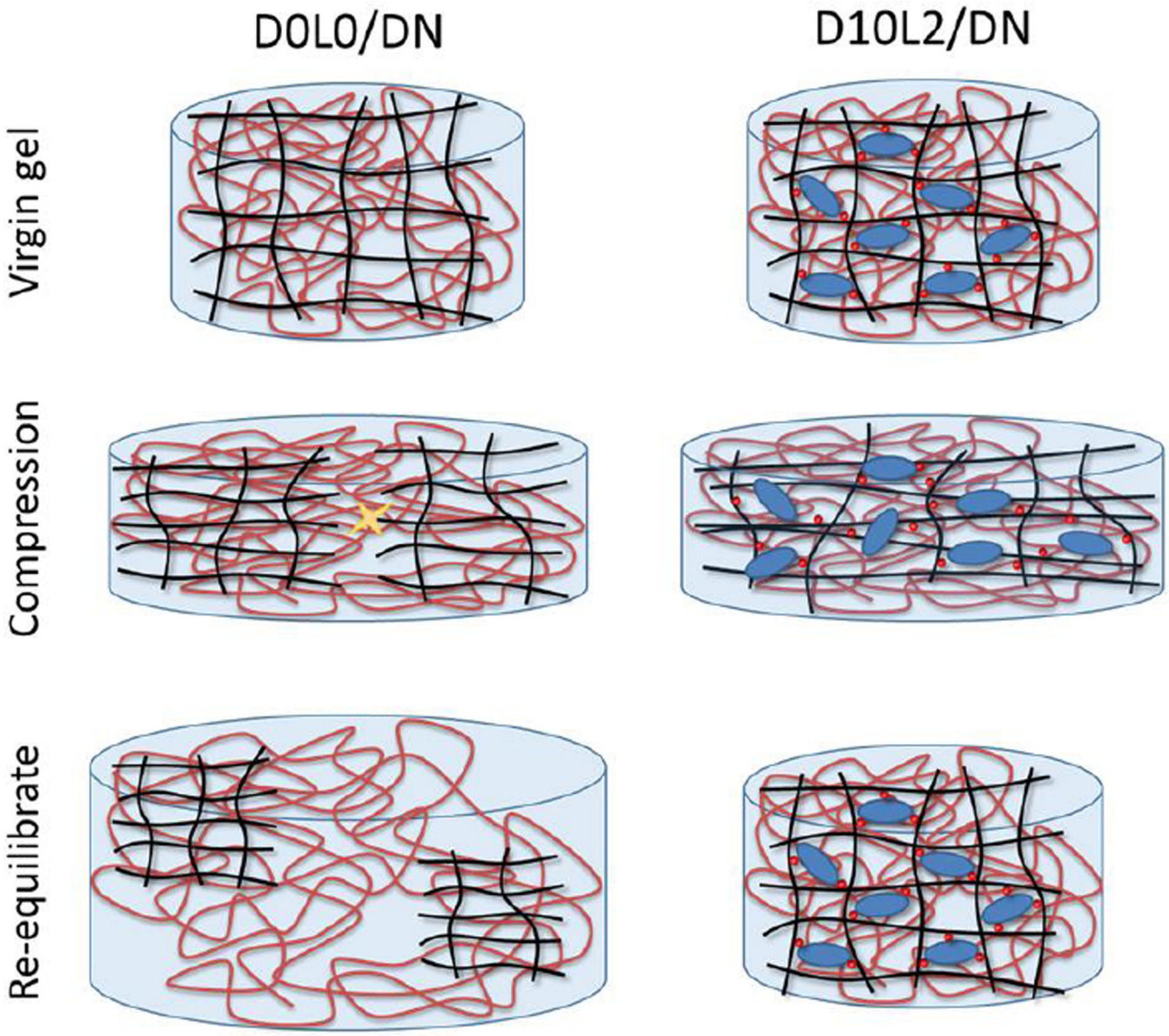

Fig. 6.

Schematic representation of DN hydrogels subjected to compression and subsequently re-equilibrated in a water bath. Compression of D0L0/DN resulted in damage to its first network and an increase in its volume after it was allowed to swell. For D10L2/DN, breaking of DMA-Laponite bonds dissipated fracture energy and the network exhibited minimal volume and structural change after the reformation of the reversible bonds. Black line: first network backbone, red line: second network backbone, red circle: catechol chemically bound to first network, blue ellipse: Laponite, yellow star mark: breaking of covalent bonds.

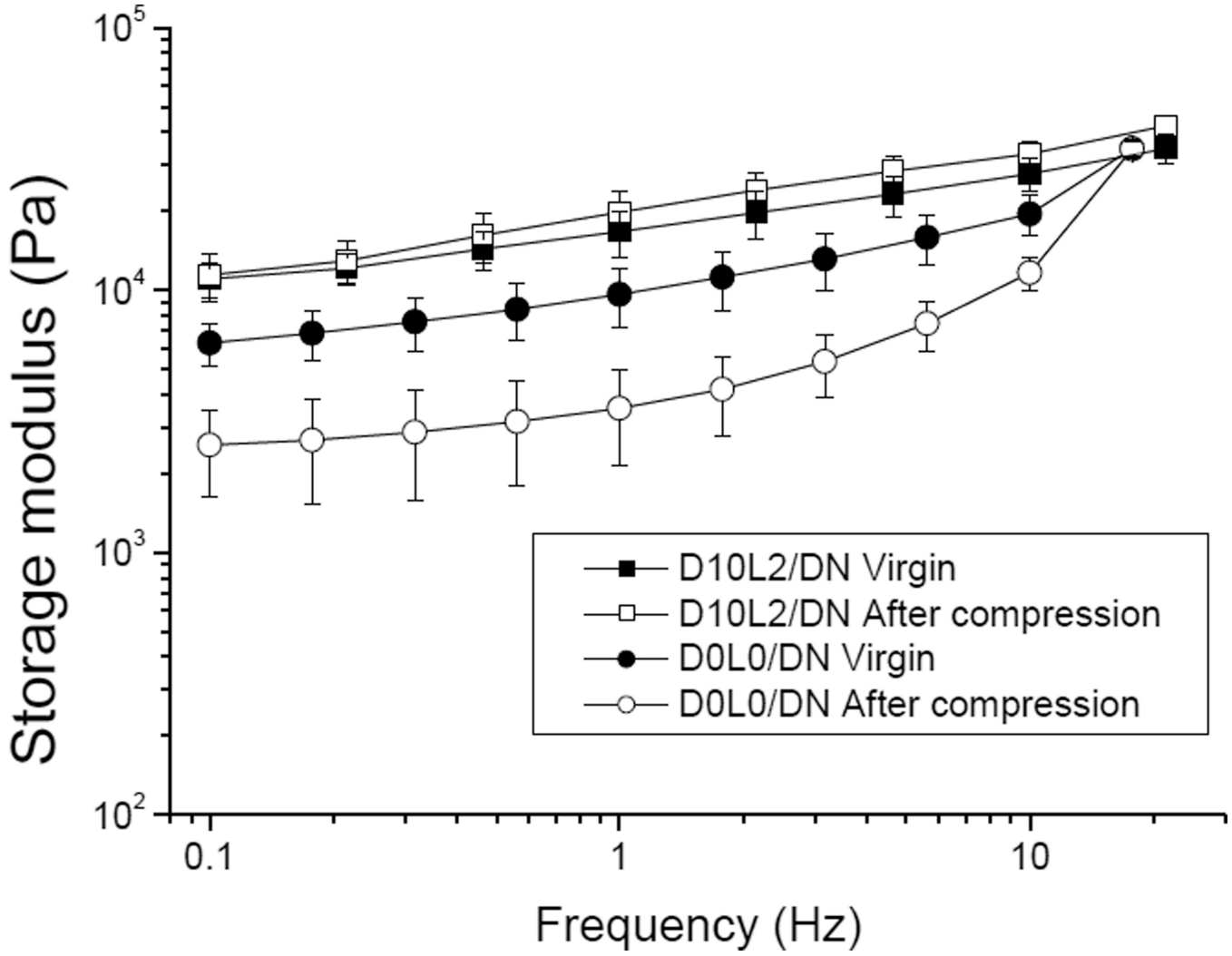

Fig. 7.

Storage modulus (G') of D0L0/DN (circles) and D10L2/DN (squares) hydrogels in the virgin state (filled symbols) and after compression to a strain of 0.5 (open symbols). Data is presented as mean ± SD (n = 3).

Table 1

Equilibrium water content (EWC) of the first network (FN) and its corresponding double network (DN), and the mass ratio between the second and first network ($\boldsymbol{R}_{\text{mass}}$).

	FN (%)	DN (%)	$\boldsymbol{R}_{\text{mass}}$
D0L0	99.1 ± 0.0854	92.3 ± 0.140	7.7
D0L2	98.9 ± 0.0591[a]	91.7 ± 0.126	6.6
D10L0	98.5 ± 0.155[a]	91.0 ± 0.392	5.1
D5L2	98.6 ± 0.221[a]	91.6 ± 0.105	5.0
D10L2	98.3 ± 0.353[a,b]	89.2 ± 0.572[a,b,d]	5.4
D10L4	97.4 ± 0.476[a,b,c]	91.2 ± 0.318	2.4

[a] $p < 0.05$ when compared to D0L0.

[b] $p < 0.05$ when compared to D0L2, D10L0, and D5L2.

[c] $p < 0.05$ when compared to D10L2.

Table 2

Strain energy and hysteresis measured for D0L0/DN and D10L2/DN after successive compressive cycles to a strain of 0.5. Data is presented as mean ± SD (n = 3)

		Strain Energy (kJ/m^3)		
		Cycle 1	Cycle 2 No wait time	Cycle 2 2 h wait time
D0L0/DN	% recovery	41 ± 1.5 -	27 ± 1.8 64%	25 ± 2.1 62%
		Hysteresis (kJ/m^3)		
		Cycle 1	Cycle 2 No wait time	Cycle 2 2 h wait time
	% recovery	20 ± 1.4 -	6.9 ± 0.52 34%	6.0 ± 0.70 32%
		Strain Energy (kJ/m^3)		
		Cycle 1	Cycle 2 No wait time	Cycle 2 2 h wait time
D10L2/DN	% recovery	61 ± 5.0 -	43 ± 1.7* 73%	58 ± 2.2 95%
		Hysteresis (kJ/m^3)		
		Cycle 1	Cycle 2 No wait time	Cycle 2 2 h wait time
	% recovery	38 ± 1.5 -	17 ± 1.7* 49%	32 ± 0.70 82%

* $p < 0.05$ when compared to 2 h wait time.